JOURNAL OF AIRCRAFT
Vol. 36, No. 4, July–August 1999

Prediction of Vortex Breakdown in Leading-Edge Vortices Above Slender Delta Wings

Z. Rusak* and D. Lamb†
Rensselaer Polytechnic Institute, Troy, New York 12180-3590

This paper applies a recent theory on the axisymmetric vortex breakdown process to experimental flow profiles of leading-edge vortices above slender delta wings at high angles of attack. Using several simplifying assumptions about the nature of the vortex generation process and its swirl ratio dependence on angle of attack, the necessary conditions for the breakdown of the vortices are calculated. The computations show agreement with the available experimental data and, thus, provide a method to predict the burst locations along a delta wing as a function of the angle of attack. Specifically, this can be predicted out of a single set of measurements at a lower angle of attack where no sign of breakdown yet exists. In addition, the calculation of the swirl ratio, based on the ratio of the maximum circumferential speed over the maximum axial speed, reveals that at the predicted breakdown conditions this parameter is almost independent of both the angle of attack and the location along the wing chord, having an average value of about 0.58. This critical value of swirl ratio may, therefore, serve as a simple criterion for the appearance of breakdown along leading-edge vortices above slender wings with sharp edges.

Nomenclature

c = wing chord length
E = variational flow force functional
$\boldsymbol{E}$ = energy functional
H = total head function
I = extended circulation
r = radial distance
r^* = normalized radial distance, r/x
r_c = vortex core radius
r_t = tube radius
U_∞ = freestream velocity
u = radial velocity component
v = circumferential velocity component
w = axial velocity component
x = axial distance from wing apex
y = square of radial distance, $r^2/2$
z = normal distance
α = angle of attack
α_{BD} = breakdown angle of attack
Λ = wing sweep angle
ψ = stream function
ω = vortex swirl ratio, v_{max}/w_{max}

I. Introduction

MODERN high-performance flight vehicles, especially fighter aircraft designed for transonic and supersonic flight, often require combinations of slender bodies and thin, swept-back lifting surfaces with sharp leading and trailing edges. These configurations generate at high angles of attack considerable aerodynamic lift forces, largely because of the induced flow generated by the vortices that are shed from the lifting surfaces and the nose of the configuration. Increasingly, the desire to improve the performances of such rapidly maneuvering vehicles to high-g maneuvers has lead to the widening of their operational envelope of flight to even higher angles of attack. Therefore, understanding and predicting the aerodynamic and flow characteristics around such configurations at high angles of attack becomes essential for their operation and the design of future vehicles.

The flowfield around a slender swept wing changes significantly with the angle of attack α. At relatively low angles, $\alpha < \sim 5$ deg, the viscous shear layers shed from the leading edges are confined to small separation zones attached to the surfaces with only small effects on the wings linear aerodynamic characteristics. Linear theories and numerical methods can be used to evaluate the aerodynamic behavior of the wings (see, e.g., Ref. 1, Chaps. 4 and 5, for an overview of this subject). As the angle of attack increases to moderate angles, ~ 5 deg $< \alpha < \sim 12$ deg, the separated layers detach from the surface into the flow as vorticity sheets that then roll up into two concentrated vortices with strong axial jets above the wing upper surface, known as the leading-edge vortices. These vortices induce additional, nonlinear lift force on the wing, and modern computational methods must be used to evaluate their behavior (see Ref. 1, Chaps. 6–9). At a higher angle of attack, however, the cores of the concentrated vortices may suddenly burst near the wing trailing edge at a certain critical wing incidence. This phenomenon is called vortex breakdown or burst and it was first found in the experiments of Peckham and Atkinson[2] (see also Lambourne and Bryer[3]). Further increase of α results in the displacement of the breakdown zone along the vortex axis toward the wing apex.[4–13]

Vortex breakdown is a basic phenomenon in fluid dynamics that refers to the sudden and significant change in the structure of swirling flows with a high level of swirl. The breakdown phenomenon is characterized by the sudden appearance of a free stagnation point (the breakdown point) along the vortex centerline, followed by a rapid dilatation of the vortical structure, regions of flow reversal, and the occurrence of large-scale fluctuations. The breakdown zone typically appears in the form of either a near-axisymmetric bubble with a helical tail, a spiral, a double-helix, or an open axisymmetric separation zone. At very high Reynolds numbers the open axisymmetric separation zone dominates. The other flow structures can be found at lower Reynolds numbers. When the breakdown point occurs above and in front of the wing mid-chord, it significantly affects the induced flowfield around the wing, causes the loss of the lift force, and leads to its stall.[2–11] This limits the envelope of flight of the aircraft. The breakdown phenomenon may also be unsteady or asymmetric,[2,3,12] and therefore can result in the appearance of undesired asymmetric loading, lateral forces and moments, and can significantly affect the stability of flight of the vehicle. The various physical, aerodynamic, and control aspects of vortex breakdown in leading-edge vortices are summarized in the review paper by Delery.[13]

Received 7 July 1998; revision received 12 April 1999; accepted for publication 13 April 1999.

*Associate Professor, Department of Mechanical Engineering, Aeronautical Engineering and Mechanics. Senior Member AIAA.
†Graduate Student, Department of Mechanical Engineering, Aeronautical Engineering and Mechanics.

The interest in expanding the flight envelope and improving the performance of aircraft has led to many experimental, numerical, and theoretical studies that attempted to understand the vortex breakdown phenomenon. The experimental works include studies of the burst location for a flow over various slender delta wings.[4–13] Based on previous experiments,[4–9] Figs. 23 and 24 in O'Neil et al.[9] summarized the measured burst locations from the wing apex as a function of angle of attack for two typical delta wings with sweep angles of $\Lambda = 60$ and 70 deg, respectively. A similar summary is also presented in Ref. 13, Fig. 24, and in Ref. 14, Fig. 3.76. As the angle of attack is increased, the breakdown point moves upstream along the vortex axis. There is some scattering in the location of the breakdown point, on the order of the vortex core diameter. This may result from either the different bluntness of the leading edge of the wing used in each experiment, the specific criterion used to select the breakdown point, the unsteady oscillations of the breakdown zone, or the effects of wind-tunnel blockage because some of the experiments were performed in wind tunnels too small for the size of the model.

Delery[13] demonstrated the two main parameters influencing the breakdown phenomenon. The first parameter is the vortex swirl intensity (or swirl ratio), which cannot increase above a critical limit. The second is the adverse pressure gradient to which the vortex is submitted, which creates a retardation effect on the axial velocity profile. The interaction between the two parameters showed that the critical limit of swirl decreases with the increase of the adverse pressure gradient (see Fig. 20 in Ref. 13). Note, however, that the critical swirl ratio approaches a certain value in the limit of zero adverse pressure gradient. Delery[13] also stated that in the case of high Reynolds number flows the breakdown of leading-edge vortices over slender wings with sharp edges is only weakly influenced by the Reynolds number.

The numerical studies of vortex breakdown above delta wings include analyses by Hoeijmakers,[15] Agrawal et al.,[16] Robinson et al.,[17] and Visbal.[18] Advanced numerical methods are able to simulate laminar flow with vortex breakdown using both the Euler and Navier–Stokes equations. However, the simulation of flow states at high Reynolds numbers on the order of 10^7, which are typical of the experimental situations and flight conditions, is still a challenging problem. Based on extensive numerical simulations, Robinson et al.[17] proposed an ad hoc Rossby number criterion, $Ro = U/r_c\Omega$ (the inverse of the swirl ratio), for locating breakdown in leading-edge vortices. (Here U is an averaged core axial speed, r_c is an effective vortex core radius, and Ω is an averaged rotation rate.) Breakdown will appear along the vortex when the local Ro falls between 0.9 and 1.4. The vortex is stable when the local Ro is above this range and always bursts when Ro is below this range.

Traub[19,20] has recently proposed several semi-empirical models to predict the location of vortex breakdown above slender wings and its variation with incidence. The methods are based on the Sychev similarity parameter to estimate the circulation along the leading-edge vortices. Although these methods show a good agreement with the experimental data, they have no theoretical basis and neglect the effects of several parameters characterizing the leading-edge vortices, such as the vortex core radius and the axial flow acceleration along the vortex axis, that strongly influence the breakdown process.

Brandt[21] has also suggested a semi-empirical model to compute the leading-edge vortex bursting trajectories with angle of attack. The model is based on analysis of a simplified version of the Navier–Stokes equations for a slender vortex together with vortex lattice method solutions. A control parameter was adjusted to experimental data. Again, the method results in good agreement with experiments but is not based on a theory that explains the vortex breakdown phenomenon.

Mahesh[22] analyzed breakdown conditions of a compressible vortex flow. His analysis is based on the ad hoc hypothesis, with no theoretical basis, that breakdown is the result of the competing effects of adverse pressure gradient and streamwise momentum flux along the vortex centerline. This analysis may apply to supersonic flows and shock-induced breakdown. However, in the case of an incompressible free vortex flow, the prediction gives a too high critical swirl ratio with respect to those found in simulations or experiments.

Theoretical analyses of vortex breakdown concentrated on an axisymmetric swirling flow in a tube or in a free domain. Several explanations were proposed: the critical-state concept,[23] the solitary trapped-wave approach,[24,25] the special state of a semi-infinite stagnation zone,[26] the analogy to boundary layer separation,[27] the nature of swirling flow states in a diverging streamtube,[28] the appearance of hydrodynamic instabilities,[29,30] and the positive feedback mechanism between the generation of negative azimuthal vorticity and the divergence of stream function surfaces.[31] Some of the approaches show a possible relationship between the axisymmetric breakdown and the critical-state concept.[23] Other approaches emphasized the importance of an adverse pressure gradient on the appearance of a separation (breakdown) zone along the vortex axis.[13]

Although much progress has been achieved in the research on the mechanisms of vortex breakdown, none of the previous theoretical or numerical tools available can be applied directly to predict the location of vortex breakdown above slender wings at high angles of attack. It was not until recently, however, that a consistent description of the complicated phenomenon of vortex breakdown has been provided.

In a recent set of papers, Wang and Rusak,[32,33] Rusak et al.,[34] Wang and Rusak,[35] Rusak et al.,[36] Rusak,[37] and Rusak et al.,[38] have presented a theoretical approach that describes the axisymmetric vortex breakdown process. The combination of various papers shows that vortex breakdown appears as a result of a nonlinear competition of effects and parameters. The main parameter is the swirl ratio characterizing the vortex flow. Other effects include the inviscid instability mechanism of vortex flows,[32–34] the viscosity,[35] the adverse pressure gradient,[36] and the upstream vorticity perturbations.[37] The theory is built of rigorous analyses of the Euler and Navier–Stokes equations that provide the various possible flow states and the stability of those states.

Because in the case of leading-edge vortices in high Reynolds number flow the viscous effects are typically small, we concentrate here on the inviscid, zero adverse pressure gradient approach of Wang and Rusak.[32,33] This approach examined the dynamics of axisymmetric swirling flows in a finite-length stream tube by applying the unsteady Euler equations. Boundary conditions that may reflect the physical situation in swirling flows in a tube were used. These conditions considered fixed in time upstream axial and swirl velocity profiles that may provide a realistic description of the flow state immediately downstream of a vortex generator at steady operation. The analysis[32] concentrated on studying both the growth rate of an initial perturbation in a swirling flow, as it relates to the stability characteristics of the flow, and the relationship between the time-asymptotic behavior of the flow and steady equilibrium states.

There exist two critical swirl ratios of the upstream vortex flow, ω_0 and ω_1, where $\omega_0 < \omega_1$. Concentrated vortex flows with a swirl ratio ω less than the threshold level ω_0 are unconditionally stable to any axisymmetric disturbance. In the range $\omega_0 < \omega < \omega_1$ the flow may evolve into one of two steady states, depending on the size of the initial disturbances. When the disturbances are sufficiently small they decay in time and the flow returns to be columnar, but when the disturbances are large they grow and evolve into a large and steady semi-infinite stagnation zone, similar to the breakdown states found in high Reynolds number turbulent flows. When $\omega > \omega_1$, any initial disturbance grows and the vortex always evolves into a stable and steady breakdown zone. Also, stable axisymmetric breakdown zones exist only when $\omega > \omega_0$. These become unstable and the flow returns to a concentrated vortex state when $\omega < \omega_0$.

These special stability characteristics are related to the propagation upstream of both small- and large-amplitude disturbances and their interaction with the fixed flow conditions downstream of the vortex generator. The disturbances tend to propagate upstream with a speed that increases with ω. When $\omega < \omega_1$, small disturbances are convected downstream by the axial flow and the concentrated vortex is, therefore, stable. However, when $\omega > \omega_1$, small disturbances tend to move upstream. Because the flow out of the vortex generator at steady operation is fixed, the disturbances cannot move through it. They are trapped, grow in time, and stabilize as a large and steady stagnation zone. These large-amplitude breakdown zones also tend

to move upstream as ω increases and can exist at swirl ratios even below ω_1. However, when $\omega < \omega_0$, these zones are convected downstream by the axial flow and the flow returns to a concentrated vortex state. Therefore, ω_0 is a threshold swirl level for breakdown states and $\omega > \omega_0$ is a necessary condition for a steady and stable axisymmetric breakdown. Also, $\omega > \omega_1$ is a sufficient condition for breakdown. For more details of the theory see Wang and Rusak[32,33] and Rusak et al.[34,38]

The effect of an adverse pressure gradient on the flow dynamics described in the previous paragraph was studied in Rusak et al.[36] It was found that when the tube divergence, or adverse pressure gradient, is smaller than a limit level, which depends on the base vortex flow profile, the inviscid instability mechanism of Wang and Rusak[32,33] is still dominant. Then, the necessary condition for breakdown remains the same as above, $\omega > \omega_0$. However, when the adverse pressure gradient is greater than the limit level, it becomes more dominant. Then, breakdown first appears at a swirl ratio, $\omega_{0\sigma}$, below ω_0 where $\omega_{0\sigma}$ is a nonlinear function of the pressure gradient. As can be seen later from the figures in Section III, in the case of a flow over a delta wing, with no compression effects behind it, there is a relatively small adverse pressure gradient along the leading-edge vortices at angles of attack before breakdown appears, or ahead of the breakdown point, at angles of attack where breakdown appears. In the present paper we assume that the adverse pressure gradient is relatively low or around the limit level and using the criterion $\omega > \omega_0$ can still provide a relevant prediction of the first appearance of a breakdown state at any point along the wing.

Although the theory[32–38] concentrates only on axisymmetric vortex flows in a stream tube (confined flows), existing experimental results[2–12] and numerical simulations[14–18] provide several strong indications that the breakdown process of leading-edge vortices above slender wings (unconfined flows) has a similar behavior. First, the fixed upstream axial and swirl velocity profiles are also relevant to the nature of the leading-edge vortices above delta wings before breakdown appears or ahead of the breakdown point. The same amount of vorticity is continuously generated and shed from the sharp edges and rolls into the vortices, independent of the dynamics of any perturbation downstream. Second, the vortices' swirl ratio may increase along the wing chord because more vorticity rolls into the vortices. Third, as the angle of attack increases, more vorticity is shed from the edges and the vortices' swirl ratio also increases. Fourth, the relatively noisy flow environment around the wing always generates sufficiently large-amplitude perturbations such that a transition to breakdown will occur immediately as the threshold swirl ratio ω_0 is reached at a certain location. Fifth, as the wing sweep-back angle increases the vortices become more concentrated and near axisymmetric. From these arguments it may be concluded that the interaction between the propagation upstream of perturbations along the vortex core, which are driven by the swirl level, and the continuous generation of the vortices from the sharp leading edges, reaches a critical balance at a threshold swirl ratio. This critical swirl ratio corresponds to a critical angle of attack and breakdown suddenly occurs for the first time near the wing trailing edge. As the angle of attack continues to increase the threshold swirl is reached at a more upstream location and, therefore, the breakdown zone moves upstream and dominates the separated flow above the wing. When the angle of attack is below the critical level all of the perturbations are convected downstream by the axial flow and the vortices are stable.

Moreover, recent calculations based on the theory[32–38] for the Burgers' vortex[34] and the Q-vortex[38] show that, as the ratio r_c/r_t of the vortex core radius over the stream tube radius is reduced to zero, both the threshold for breakdown swirl ratio ω_0 and the critical swirl ω_1 approach certain finite limit values. For example, for a Q-vortex with a strong axial jet this limit threshold swirl ratio occurs when the swirl ratio $v_{\max}/w_{\max}$ of maximum circumferential speed at the core edge over maximum axial speed at the core center is about 0.6. This limit case may also apply by analogy to the behavior of a finite core vortex in an infinite tube or a partially bounded vortex, such as the leading-edge vortex above a slender delta wing. Specifically, calculation of the threshold swirl ratio ω_0 for an experimental vortex state at a certain cross section along the wing chord, as if it is inserted in a large radius tube, may provide a relevant prediction of the swirl ratio or angle of attack at which breakdown appears at that location.

The objective of this paper is to use the new theory of Wang and Rusak[32] as a framework to conduct computations of the breakdown process in leading-edge vortices. Altough the theory is limited to the inviscid and zero adverse pressure gradient approach, it may still provide relevant predictions of the location of vortex breakdown above slender delta wings. Corrections resulting from the effects of viscosity and the pressure rise along the vortex can be estimated according to the asymptotic analyses in Refs. 35 and 36 and will be investigated in the future.

The outline of this paper is as follows. In Sec. II, a summary of the method to compute ω_0 is given. This is followed by a discussion on the approach used to analyze the test data provided by O'Neil et al.[9] (Sec. III). In Sec. IV, the resulting calculated burst locations above various delta wings are computed and are compared to the test results. The paper is concluded with a summary of main results and a discussion.

II. Computation of ω_0

The method to compute ω_0 results from the nature of solutions of the Squire-Long equation (SLE) (derived from the axisymmetric, steady-state Euler equations):

$$\psi_{yy} + \psi_{xx}/2y = H'(\psi) - I'(\psi)/2y \tag{1}$$

with boundary conditions

$$\psi(x, 0) = 0, \qquad \psi\left(x, \tfrac{1}{2}\right) = \psi_0\left(\tfrac{1}{2}\right), \qquad \psi(0, y) = \psi_0(y)$$
$$K(0, y) = \omega K_0(y), \qquad \psi_x(x_0, y) = 0 \tag{2}$$

Here, r is the distance from the vortex axis rescaled with the stream tube radius r_t, $y = r^2/2$ and x_0 is the tube length. The streamfunction is $\psi(x, y)$, where the axial and radial speeds are $w = \psi_y$ and $u = -\psi_x/\sqrt{(2y)}$, and $K = rv$ is the circulation function. The upstream stream function $\psi_0(y)$ and the circulation profiles $\omega K_0(y)$ are related to the axial and circumferential upstream velocity profiles $w_0(y) = \psi_{0y}(y)$ and $v_0(y) = \omega K_0(y)/\sqrt{(2y)}$. The total head function is $H = p/\rho + (u^2 + w^2 + v^2)/2$ and $I = K^2/2$ is the extended circulation; both are functions of ψ only. Solutions of the SLE correspond to the extremum points of the following energy functional[26]:

$$\boldsymbol{E}(\psi) = \int_0^{x_0} \int_0^{\frac{1}{2}} \left[\frac{\psi_y^2}{2} + \frac{\psi_x^2}{4y} + H(\psi) - \frac{I(\psi)}{2y} \right] \mathrm{d}y\, \mathrm{d}x \tag{3}$$

It has been shown[32] that the solution $\psi_g(x, y)$ that globally minimizes $\boldsymbol{E}(\psi)$ is dominated by the solution $\psi_s(y)$ of the columnar, ordinary differential equation (ODE) problem

$$\psi_{yy} = H'(\psi) - I'(\psi)/2y, \qquad \psi(0) = 0, \qquad \psi\left(\tfrac{1}{2}\right) = \psi_0\left(\tfrac{1}{2}\right) \tag{4}$$

that globally minimizes the variational columnar flow-force functional[23]

$$E(\psi) = \int_0^{\frac{1}{2}} \left[\frac{\psi_y^2}{2} + H(\psi) - \frac{I(\psi)}{2y} \right] \mathrm{d}y \tag{5}$$

As demonstrated by Wang and Rusak,[32] when ω is smaller than the threshold value ω_0, the solution of Eq. (4) that globally minimizes E is the base flow $\psi_s(y) = \psi_0(y)$. This implied that the solution of Eq. (1) that globally minimizes $\boldsymbol{E}$ is also the columnar flow $\psi_g(x, y) = \psi_0(y)$. When ω is greater than the threshold value ω_0, however, the solution of Eq. (4) that globally minimizes E is different from $\psi_0(y)$. This solution, $\psi_s(y)$, contains a separation zone and $E[\psi_s(y)] < E[\psi_0(y)]$. The solution of Eq. (1) that globally minimizes $\boldsymbol{E}$, therefore, describes a vortex breakdown state that

is a transition in space along the vortex axis from an upstream state $\psi_g(0, y) = \psi_0(y)$ to a downstream state $\psi_g(x_0, y) = \psi_s(y)$ with less columnar flow force than the inlet. The difference between $E[\psi_0(y)]$ and $E[\psi_s(y)]$ creates a radial flow along the upstream section to establish the separation (breakdown) zone. To compute the swirl threshold ω_0, therefore, it is necessary to find all of the solutions for Eq. (4) for a given ω including those with a separation zone. For each solution, the flow force according to Eq. (5) must then be computed and compared with the inlet state flow force at the same ω. The swirl threshold ω_0 for axisymmetric breakdown is found when there exists another solution, $\psi_s(y)$, of Eq. (4), other than the base upstream vortex state $\psi_0(y)$, where $E[\psi_s(y)] = E[\psi_0(y)]$. At this point, it should also be clarified that the state that globally minimizes $E(\psi)$ depends on the choice of a continuation model in the separation zone. In the computations for ω_0, a stagnation model is being used for the separation zone. This model has been selected based on the numerical unsteady inviscid flow simulations by Rusak et al.[34] that demonstrate the natural establishment of a stagnation zone in inviscid flows when ω is greater than ω_0 and as time tends to infinity.

The threshold swirl ratio for breakdown ω_0 is computed by using a program developed by Rusak et al.[38] to predict vortex breakdown of any vortex flow based on the method previously outlined. This program uses a standard differential equation solver from the Fortran routines to integrate Eq. (4) numerically for a fixed ω. The critical swirl level is found iteratively by changing ω until another solution, $\psi_s(y)$, besides the base vortex state, $\psi_0(y)$, exists for which the flow force function [Eq. (5)] equates that of the base flow. For complete details on these type of computations see Rusak et al.[34,38]

III. Analysis

The objective of this study is to develop a tool to predict vortex breakdown of leading-edge vortices over delta wings by applying the recent theory of Wang and Rusak[32] to experimental vortex profiles at various cross sections above slender delta wings. Specifically, two delta wing configurations are investigated according to the data in O'Neil et al.[9] These data consist of velocity profiles and vortex breakdown locations for a $\Lambda = 60$-deg delta wing at angles of attack of 12 and 16 deg and a $\Lambda = 70$-deg delta wing at angles of attack of 25 and 28 deg. The resulting predictions for the angle of attack at which vortex breakdown occurs at the various cross sections of these configurations are then compared to experimental test results provided by O'Neil et al.[9]

The process to generate the vortex profiles from the experimental data provided by O'Neil et al.[9] consists of the following steps. At a given angle of attack α, the vector plots of the circumferential flowfields at various cross sections x/c along the wing are constructed. A total of 14 different cases are investigated. These test cases are listed in Table 1. Figures 1 and 2 provide two typical examples of the generated vortex plots. Figure 1 is a vector plot of the

Table 1 Experimental test cases: formulas for scaled circumferential and axial velocity profiles and predicted threshold swirl ratios for vortex breakdown

Configuration	α	x/c	Circumferential velocity	Axial velocity	ω_0
$\Lambda = 60$-deg delta wing	12 deg	0.25	$v_0 = 24.15815r^* - 208.971r^{*2} + 865.2331r^{*3} - 1915.47r^{*4} + 2291.338r^{*5} - 1393.65r^{*6} + 337.5844r^{*7}$	$w_0 = 2.151797 - 53.3466r^{*2} + 278.4773r^{*3} - 598.913r^{*4} + 613.7275r^{*5} - 280.354r^{*6} + 39.45551r^{*7}$	1.901
		0.50	$v_0 = 14.17726r^* - 103.546r^{*2} + 414.548r^{*3} - 944.043r^{*4} + 1180.144r^{*5} - 751.077r^{*6} + 189.9892r^{*7}$	$w_0 = 1.812998 - 29.2689r^{*2} + 117.3035r^{*3} - 179.499r^{*4} + 100.4073r^{*5} + 11.33328r^{*6} - 20.9679r^{*7}$	1.205
		0.75	$v_0 = 13.59053r^* - 87.6469r^{*2} + 256.9933r^{*3} - 385.212r^{*4} + 287.0114r^{*5} - 83.5829r^{*6} - 0.5965r^{*7}$	$w_0 = 1.637711 - 19.9064r^{*2} + 81.16187r^{*3} - 113.092r^{*4} + 26.3762r^{*5} + 59.25878r^{*6} - 34.3325r^{*7}$	1.194
	16 deg	0.30	$v_0 = 14.45814r^* - 65.4845r^{*2} + 91.21227r^{*3} + 10.65575r^{*4} - 65.4343r^{*5} - 34.3318r^{*6} + 49.5738r^{*7}$	$w_0 = 2.207601 - 49.6271r^{*2} + 272.6924r^{*3} - 610.425r^{*4} + 625.9448r^{*5} - 261.038r^{*6} + 21.39515r^{*7}$	1.502
		0.40	$v_0 = 16.96448r^* - 110.099r^{*2} + 319.0449r^{*3} - 408.731r^{*4} + 128.8624r^{*5} + 152.4387r^{*6} - 97.8183r^{*7}$	$w_0 = 1.908591 - 19.7759r^{*2} + 105.0268r^{*3} - 311.101r^{*4} + 511.3704r^{*5} - 419.934r^{*6} + 133.5391r^{*7}$	1.160
		0.45	$v_0 = 17.18459r^* - 119.656r^{*2} + 340.8164r^{*3} - 378.996r^{*4} - 11.4097r^{*5} + 302.6664r^{*6} - 150.066r^{*7}$	$w_0 = 1.987409 - 50.9497r^{*2} + 275.8599r^{*3} - 606.258r^{*4} + 618.5342r^{*5} - 267.789r^{*6} + 29.6094r^{*7}$	1.350
		0.50	$v_0 = 13.64721r^* - 69.1866r^{*2} + 137.4292r^{*3} - 88.5286r^{*4} - 45.6983r^{*5} + 73.61962r^{*6} - 20.6327r^{*7}$	$w_0 = 1.733406 - 23.4669r^{*2} + 126.6581r^{*3} - 344.157r^{*4} + 518.5623r^{*5} - 402.263r^{*6} + 123.9396r^{*7}$	1.200
$\Lambda = 70$-deg delta wing	25 deg	0.40	$v_0 = 23.13843r^* - 145.759r^{*2} + 394.9573r^{*3} - 445.427r^{*4} + 46.14563r^{*5} + 264.8451r^{*6} - 137.179r^{*7}$	$w_0 = 2.714059 - 72.9286r^{*2} + 371.4686r^{*3} - 888.654r^{*4} + 1152.273r^{*5} - 775.383r^{*6} + 211.3557r^{*7}$	1.315
		0.60	$v_0 = 22.55463r^* - 144.055r^{*2} + 393.128r^{*3} - 452.84r^{*4} + 72.87204r^{*5} + 235.1629r^{*6} - 126.14r^{*7}$	$w_0 = 2.693056 - 75.8363r^{*2} + 377.9141r^{*3} - 864.716r^{*4} + 1056.542r^{*5} - 665.353r^{*6} + 169.5538r^{*7}$	1.200
		0.80	$v_0 = 25.98549r^* - 177.68r^{*2} + 521.6507r^{*3} - 700.869r^{*4} + 323.6724r^{*5} + 111.9215r^{*6} - 104.076r^{*7}$	$w_0 = 2.59 - 78.2186r^{*2} + 351.2256r^{*3} - 653.517r^{*4} + 570.2158r^{*5} - 202.884r^{*6} + 11.35686r^{*7}$	1.151
	28 deg	0.50	$v_0 = 23.13843r^* - 145.759r^{*2} + 394.9573r^{*3} - 445.427r^{*4} + 46.14563r^{*5} + 264.8451r^{*6} - 137.179r^{*7}$	$w_0 = 2.931809 - 60.4787r^{*2} + 259.2134r^{*3} - 723.365r^{*4} + 989.7953r^{*5} - 704.784r^{*6} + 201.5897r^{*7}$	1.195
		0.65	$v_0 = 25.4731r^* - 172.463r^{*2} + 489.8209r^{*3} - 587.71r^{*4} + 122.0262r^{*5} + 281.3912r^{*6} - 157.88r^{*7}$	$w_0 = 2.702698 - 45.3788r^{*2} + 192.1743r^{*3} - 426.151r^{*4} + 563.0339r^{*5} - 404.573r^{*6} + 119.068r^{*7}$	1.100
		0.70	$v_0 = 28.19476r^* - 185.064r^{*2} + 509.8763r^{*3} - 597.924r^{*4} + 124.4903r^{*5} + 273.3053r^{*6} - 152.148r^{*7}$	$w_0 = 2.778486 - 63.8007r^{*2} + 274.6848r^{*3} - 536.144r^{*4} + 550.7256r^{*5} - 285.445r^{*6} + 57.99719r^{*7}$	1.091
		0.75	$v_0 = 31.29911r^* - 205.906r^{*2} + 560.0224r^{*3} - 653.682r^{*4} + 152.404r^{*5} + 268.8749r^{*6} - 152.348r^{*7}$	$w_0 = 2.920181 - 81.3842r^{*2} + 389.4885r^{*3} - 848.967r^{*4} + 983.4362r^{*5} - 585.492r^{*6} + 140.8374r^{*7}$	1.089

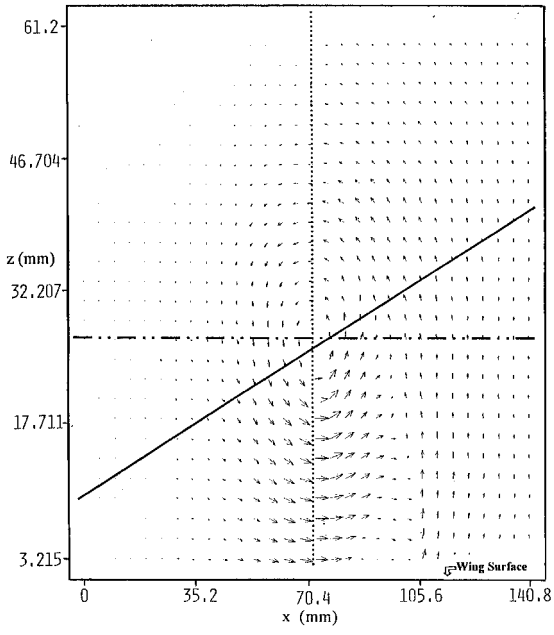

Fig. 1 Vector plot of the circumferential velocity for the $\Lambda = 60$-deg delta wing at an angle of attack of 16 deg and at $x/c = 0.3$.

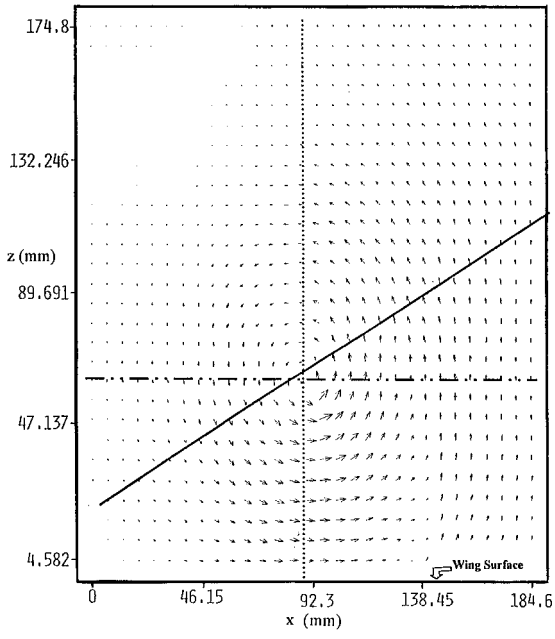

Fig. 2 Vector plot of the circumferential velocity for the $\Lambda = 70$-deg delta wing at an angle of attack of 28 deg and $x/c = 0.5$.

circumferential velocity for the $\Lambda = 60$-deg delta wing at an angle of attack of 16 deg and at $x/c = 0.3$. Figure 2 is the vector plot of the circumferential velocity for the $\Lambda = 70$-deg delta wing at an angle of attack of 28 deg and $x/c = 0.5$. Vector plots for all of the other cases studied are generated in a similar way and can be found in Lamb.[39]

The leading-edge vortex flow is evident from the vector plots. In addition, it can also be seen from both figures that the upper wing surface has a significant effect on the circumferential velocity. This effect increases as the vortex gets closer to the surface of the wing as the wing apex is approached or when the wing sweep-back angle Λ is reduced. O'Neil et al.[9] demonstrated that for slender delta wings with $\Lambda \geq 70$ deg the leading-edge vortices are near axisymmetric along most of the wing chord but as the wing sweep back angle decreases below 65 deg the vortex deviates from an axisymmetric profile. To minimize the effect of the wing surface the vortex profile along an inclined transverse cut is used in this analysis. Such cuts are shown as the solid black lines in both examples in Figs. 1 and 2. The vortex profile along the cut may be considered as an averaged axisymmetric profile that corresponds to the leading-edge vortex at a certain cross section.

Using the minimum least-squares method, analytical formulas are curved fit to the measured axial and circumferential velocity profiles along each cut. These are functions of the radial position along the transverse cut, normalized with the chordwise position along the wing, $r^* = r/x$. Both velocities are rescaled with the freestream velocity U_∞. Special attention is given to the accurate representation of the swirl profile at the vortex viscous subcore. Also notice that, for simplicity, we rescale the swirl parameter ω such that at each cross section $\omega = 1$. The formulas describing the various rescaled profiles for the axial velocity $w_0(r^*)$ and circumferential velocity $v_0(r^*)$ are summarized in Table 1. Note that both the axial and circumferential velocity profiles are usually approximated by seventh-order polynomial functions.

Figures 3a and 3b show typical profiles of the axial speed $w_0(r^*)$ and circumferential speed $v_0(r^*)$ curve fit formulas at certain angles

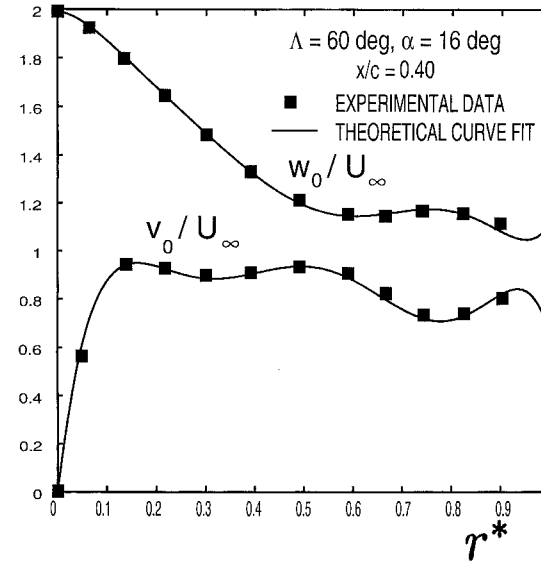

Fig. 3a Axial and circumferential velocity curve fit profiles to the experimental results[9] for $\Lambda = 60$ deg, $\alpha = 16$ deg, and $x/c = 0.4$.

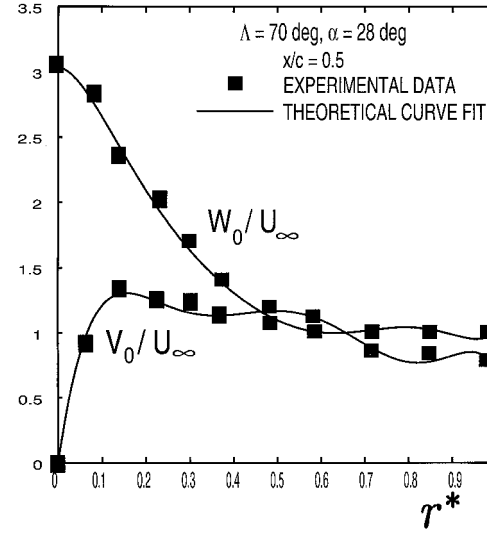

Fig. 3b Axial and circumferential velocity curve fit profiles to the experimental results[9] for $\Lambda = 70$ deg, $\alpha = 28$ deg, and $x/c = 0.5$.

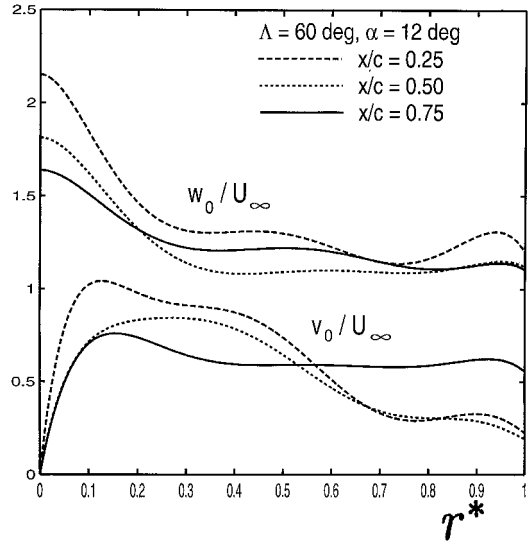

Fig. 4 Axial and circumferential velocity curve fit profiles to the experimental results[9] along Λ = 60-deg delta wing at α = 12 deg.

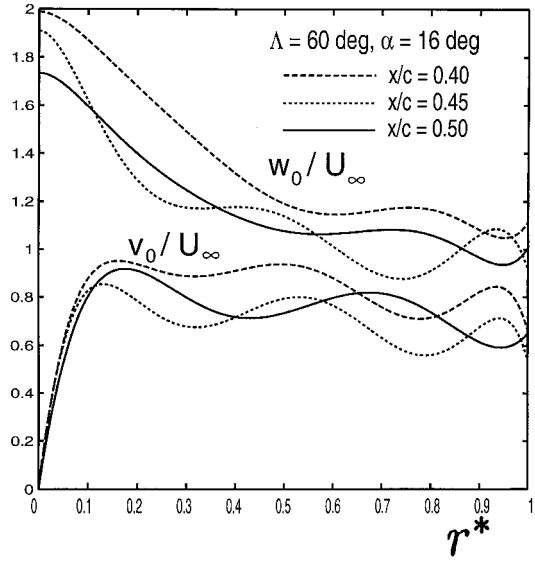

Fig. 5 Axial and circumferential velocity curve fit profiles to the experimental results[9] along Λ = 60-deg delta wing at α = 16 deg.

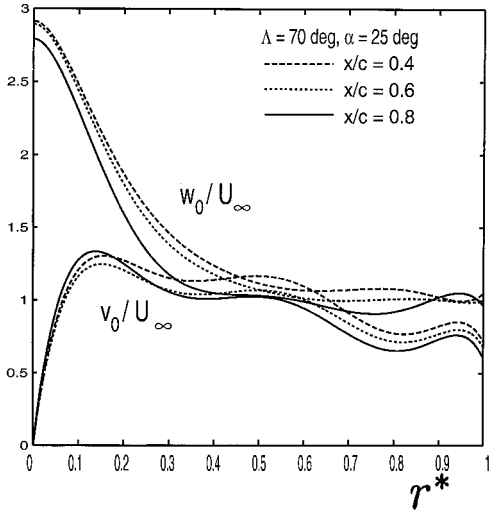

Fig. 6 Axial and circumferential velocity curve fit profiles to the experimental results[9] along Λ = 70-deg delta wing at α = 25 deg.

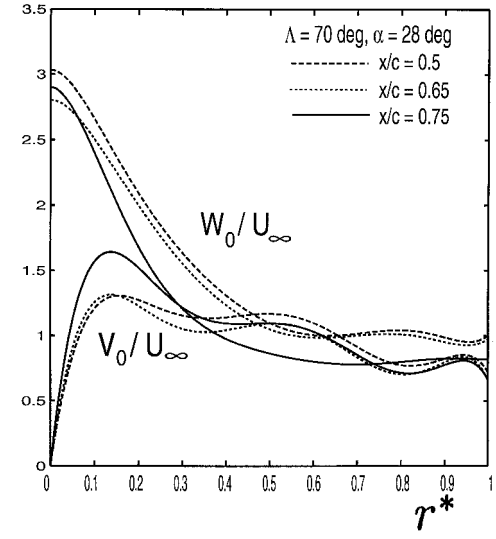

Fig. 7 Axial and circumferential velocity curve fit profiles to the experimental results[9] along Λ = 70-deg delta wing at α = 28 deg.

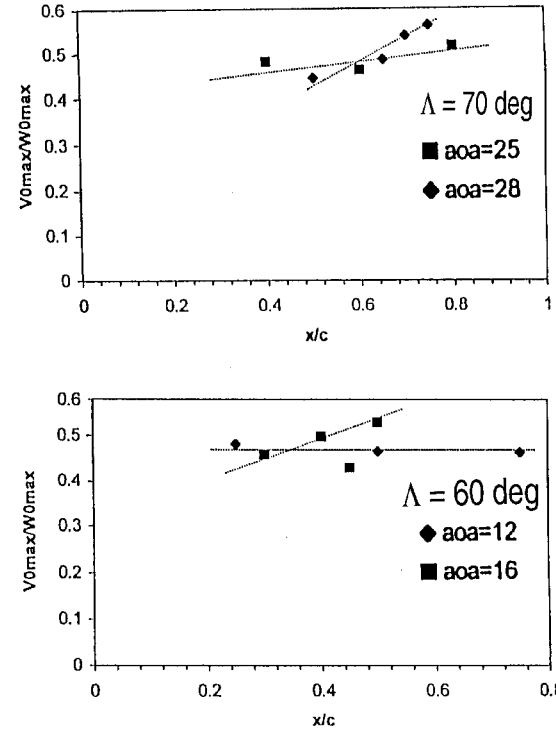

Fig. 8 Swirl ratio $v_{0\,\max}/w_{0\,\max}$ as a function of x/c for various angles of attack, α, and delta wings.

of attack and chordwise locations for both the Λ = 60- and 70-deg delta wings, respectively. These figures demonstrate the agreement between the computed profiles and the experimental data. Figures 4–7 show the computed axial and circumferential velocity profiles at various angles of attack and cross sections along the Λ = 60- and 70-deg delta wings. It can be seen that both the axial and circumferential velocities have higher values for the Λ = 70-deg delta wing than for the Λ = 60-deg delta wing. Also, in general, the swirl ratio $v_{0\,\max}/w_{0\,\max}$ (ratio of maximum circumferential speed at the edge of the vortex core over maximum axial speed at the vortex axis) increases as both x/c or α are increased (see Fig. 8).

Figures 4–7 also show that, for all cases, the axial speed deceleration along the vortex axis is relatively small. This indicates that the leading-edge vortices are subjected to a relatively small adverse pressure gradient before breakdown appears, as assumed in the present analysis.

For each one of the vortex profiles $w_0(r^*)$ and $v_0(r^*)$ defined, the threshold for breakdown swirl ratio ω_0 is calculated according to the method described in Sec. II. It is assumed that each of the vortex states is given in a circular tube where the vortex core radius over the tube radius $r_c/r_t = 0.05$. Computations with this ratio of r_c/r_t result in values of ω_0 within 2% of the limit value as r_c/r_t tends to zero. The results for ω_0 are also summarized in Table 1. It can be seen that $\omega_0 > \omega = 1$ for each Λ, α, and x/c. This means that each one of the vortex profiles studied is, indeed and as expected, absolutely stable and cannot suffer breakdown at the specific conditions it is given at because its swirl ratio ($\omega = 1$) is below the threshold for breakdown at these conditions.

IV. Results

Although the above-mentioned vortex profiles are stable, we can now use the information for their ω_0 to predict the angle of attack α_{BD} at which, for a given Λ and x/c, the threshold swirl ratio is achieved and breakdown occurs. We assume that as α is increased the vortex profiles are fixed for each wing and at each cross section x/c. The only effect of α is increasing the swirl ratio ω in an approximately linear relation, $\omega \sim \alpha$. Therefore, the vortex breakdown angle of attack at that cross section may be estimated by

$$\alpha_{BD} = (\omega_0/\omega)\alpha \tag{6}$$

where according to the preceding formulas $\omega = 1$ at each cross section. Table 2 presents the predicted angles of attack for each of the test cases. Figures 9 and 10 show a comparison of the calculated vortex breakdown locations as function of α_{BD} (based on the data from Ref. 9) with the actual experimental results.[9] In Fig. 9 (delta wing with $\Lambda = 60$-deg), the solid square points are based on analysis of profiles at $\alpha = 12$ deg and the solid triangle points on profiles at $\alpha = 16$ deg. Similarly, in Fig. 10 (delta wing with $\Lambda = 70$ deg), the solid square points are based on analysis of profiles at $\alpha = 25$ deg and the solid triangle points on profiles at $\alpha = 28$ deg. Also shown in Fig. 9 and 10, for reference, are the experimental results from

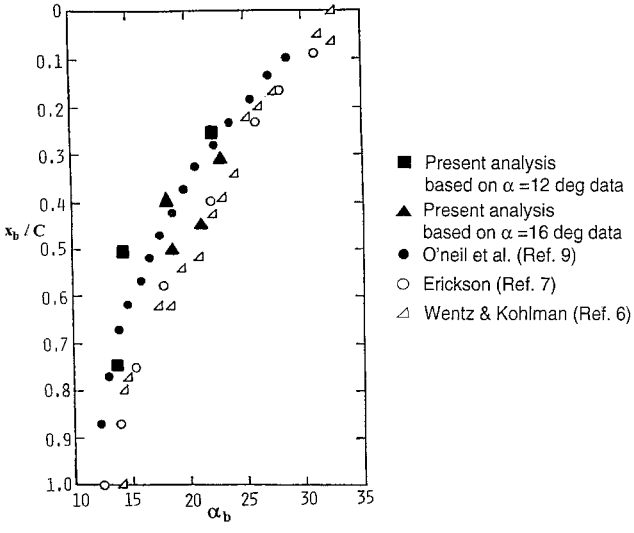

Fig. 9 Comparison of the calculated vortex breakdown locations as a function of α_{BD} with the experimental results[9] ($\Lambda = 60$-deg delta wing) and other available data.

Table 2 Predicted breakdown angles of attack and swirl ratio for each of the test cases

Delta wing configuration	α	x/c	ω_0	α_b, deg	$(V_{0\max}/W_{0\max})_b$
$\Lambda = 60$-deg delta wing	12 deg	0.25	1.901	22.81	0.92
		0.50	1.205	14.46	0.56
		0.75	1.194	14.33	0.55
	16 deg	0.30	1.502	24.03	0.69
		0.40	1.160	18.56	0.58
		0.45	1.350	21.60	0.58
		0.50	1.200	19.20	0.64
	25 deg	0.40	1.315	32.88	0.63
		0.60	1.200	30.00	0.56
		0.80	1.151	28.78	0.59
$\Lambda = 70$-deg delta wing	28 deg	0.50	1.195	33.46	0.53
		0.65	1.100	30.80	0.53
		0.70	1.091	29.43	0.57
		0.75	1.089	30.49	0.61
$\Lambda = 75$-deg delta wing	29 deg	0.50	1.328	38.43	0.65

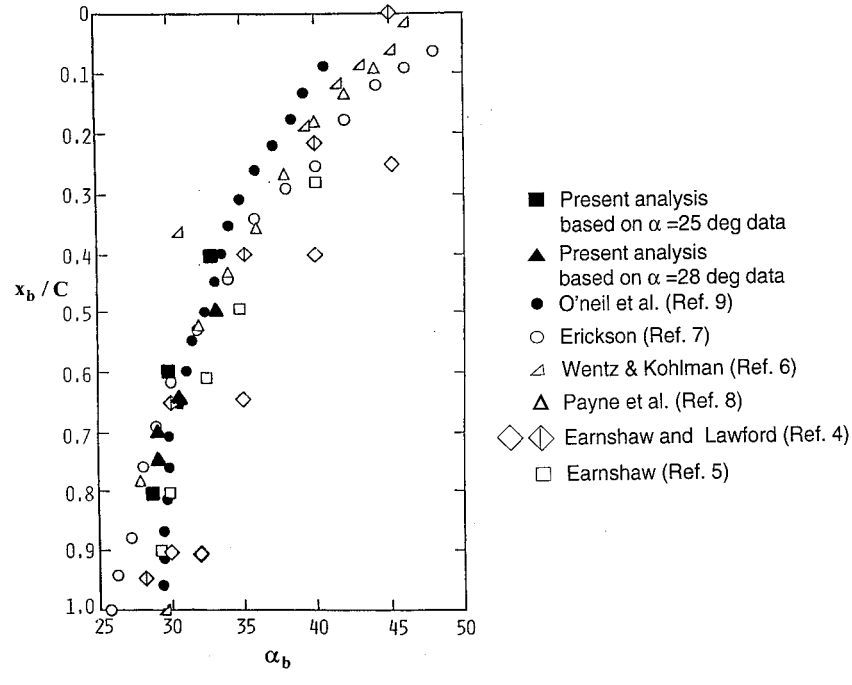

Fig. 10 Comparison of the calculated vortex breakdown locations as a function of α_{BD} with the experimental results[9] ($\Lambda = 70$-deg delta wing) and other available data.

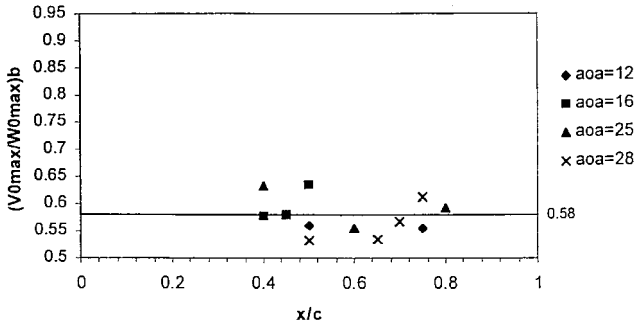

Fig. 11 Breakdown swirl ratios for the various test cases studied.

several additional sources[4–8] that demonstrate the scattering in the measurement of the breakdown location.

Examination of Figs. 9 and 10 shows a fair agreement between the theoretically calculated breakdown locations and those reported in O'Neil et al.[9] (the solid circles) for both the $\Lambda = 60$- and 70-deg delta wings. These results demonstrate that, given a single set of measurements at a certain angle of attack where vortex breakdown did not even appear anywhere above the entire wing (such as the vortex states along the $\Lambda = 60$-deg delta wing at $\alpha = 12$ deg or along the $\Lambda = 70$-deg delta wing at $\alpha = 25$ deg), the vortex burst locations at various axial positions along the wing as a function of angle of attack can be predicted using the theoretical approach of Wang and Rusak.[32] The results demonstrate the ability of the theory to predict the abrupt and sudden nature of the breakdown process that could not be predicted by any of the previous theoretical works.

There is some noticeable difference between the consistency of the theoretical results for the two delta wing configurations that may partly be explained by the effect of the wing surface on the generated vortex. For the $\Lambda = 60$-deg delta wing, the leading-edge vortex is much closer to the wing upper surface. The wing, therefore, has a much greater effect on this vortex. This is evident by a comparison of Figs. 1 and 2. The increased interference with the wing decreases the axisymmetry of the vortex flow, making the averaged vortex model used in the analysis not as representative of the flow. In each case, however, the results demonstrate that the vortex burst location can be predicted.

Also included in Table 2 are the calculated values of the swirl ratios at the breakdown conditions according to the formula

$$\left(\frac{v_{0\max}}{w_{0\max}}\right)_{\mathrm{BD}} = \frac{\omega_0}{\omega}\frac{v_{0\max}}{w_{0\max}} \tag{7}$$

Figure 11 shows the various calculated breakdown swirl ratios, $(v_{0\max}/w_{0\max})_{\mathrm{BD}}$ for the $\Lambda = 60$-deg and the $\Lambda = 70$-deg delta wings. Examination of Fig. 11 reveals that the breakdown swirl ratios are almost independent of both Λ and x/c, having an average value of 0.58 ± 0.03. (Note that the points for $\Lambda = 60$-deg delta wing at $\alpha = 12$ deg and $x/c = 0.25$ and at $\alpha = 16$ deg and $x/c = 0.3$ with values above 0.7 are neglected as outlying points.) This implies that the parameter $(v_{0\max}/w_{0\max})_{\mathrm{BD}}$ may serve as a universal criterion for the appearance of breakdown in leading-edge vortices. At any point along the leading-edge vortex where the swirl ratio reaches the critical value $(v_{0\max}/w_{0\max})_{\mathrm{BD}} = 0.58 \pm 0.03$ vortex breakdown appears. Notice that this critical value also matches the threshold swirl ratio of about 0.6 of Q-vortices with a strong jet when the vortex core radius over tube radius approaches zero.[38]

V. Summary and Discussion

This paper presents calculations for the angle of attack where vortex breakdown occurs above various delta wings. These calculations are guided by the recent inviscid theory of Wang and Rusak[32] on vortex breakdown in a finite-length tube with a zero pressure gradient along it. A certain limit process of the vortex core radius to the tube radius tending to zero is applied. The resulting predicted breakdown angles of attack show fair agreement with experimental data on burst location for various slender delta wings. Calculations based on this theory, therefore, can be used to predict the burst locations along a delta wing from a single set of measurements at a given angle of attack, specifically, from a data set where breakdown did not even appear anywhere in the flowfield around the wing.

In addition, calculation of the swirl ratio at the breakdown conditions, $(v_{0\max}/w_{0\max})_{\mathrm{BD}}$, for each of the test cases reveals that this parameter is almost independent of both the angle of attack α and location along the wing x/c, having an average value of 0.58 ± 0.03. This swirl ratio, therefore, may serve as a universal criterion for the appearance of breakdown along leading-edge vortices. At any point along the leading-edge vortex where the swirl ratio reaches the critical value 0.58 vortex breakdown will appear.

It should be noted that the predicted angles of attack for breakdown are more consistent with the experimental results when the wing is more slender (higher sweep back angle Λ). This is probably because the current theory of Wang and Rusak[32] is limited to axisymmetric swirling flow. Because the leading-edge vortex is located much closer to the wing surface when the delta wing is less slender, the effect of the wing on the vortex structure is stronger and the vortex deviates from axisymmetry. The analysis assumption of axisymmetric flow becomes less accurate and the theory[32] may not describe the vortex breakdown process as accurately.

The effect of the adverse pressure gradient along the vortex axis on the breakdown conditions may also play an important role (see Ref. 13) and should be investigated. It is proposed to use the asymptotic theory of Rusak et al.[36] for computing these conditions. The comparison of results between such computations and the present study will help to clarify the nonlinear interaction between the vortex swirl ratio and the pressure rise along the vortex.

Acknowledgments

The authors would like to thank Fredrick W. Roos from The Boeing Company, St. Louis, Missouri, for providing the detailed experimental data related to Refs. 9–11 and for many interesting discussions on the subject. This research was carried out with the support of the National Science Foundation under Grant CTS-9804745.

References

[1]Rom, J., *High Angle of Attack Aerodynamics,* Springer–Verlag, New York, 1992.

[2]Peckham, D. H., and Atkinson, S. A., "Preliminary Results of Low Speed Wind Tunnel Tests on a Gothic Wing of Aspect Ratio 1.0," Aeronautical Research Council, TR CP508, London, 1957.

[3]Lambourne, N. C., and Bryer, D. W., "The Bursting of Leading-Edge Vortices—Some Observations and Discussion of the Phenomenon," Aeronautical Research Council, Rept. No. 3282, London, 1962, pp. 1–36.

[4]Earnshaw, P. B., and Lawford, J. A., "Low-Speed Wind-Tunnel Experiments on a Series of Sharp-Edged Delta Wings," Aeronautical Research Council, Rept. No. 3424, London, 1964.

[5]Earnshaw, P. B., "Measurements of the Effects of Thickness on Vortex Breakdown Position on a Series of Sharp-Edged Delta Wings," Aeronautical Research Council, TR CP 1018, London, 1968.

[6]Wentz, W. H., and Kohlman, D. L., "Vortex Breakdown on Slender Sharp-Edged Wings," *Journal of Aircraft,* Vol. 8, No. 3, 1971, pp. 156–161.

[7]Erickson, G. E., "Flow Studies of Slender Wing Vortices," AIAA Paper 80-1423, 1980.

[8]Payne, F. M., Ng, T. T., Nelson, R. C., and Schiff, L. B., "An Investigation of Vortex Breakdown on a Delta Wing at High Angles of Attack," AIAA Paper 83-2114, 1983.

[9]O'Neil, P. J., Roos, F. W., Barnett, R. M., and Hawk, J. D., "Investigation of Flow Characteristics of Developed Vortex," McDonnell Aircraft Company, Rept. NADC-89114-60, St. Louis, MO, 1989.

[10]Roos, F. W., and Kegelman, J., "An Experimental Investigation of Sweep-Angle Influence on Delta Wing Flows," AIAA Paper 90-0383, Jan. 1990.

[11]Kegelman, J., and Roos, F. W., "The Flow Fields of Bursting Vortices over Moderately Swept Delta Wings," AIAA 28th Aerospace Sciences Meeting and Exhibit, AIAA Paper 90-0599, Reno, NV, Jan. 1990.

[12]Menke, M., and Gursul, I., "Unsteady Nature of Leading-Edge Vortices," *Physics of Fluids,* Vol. 9, No. 10, 1997, pp. 2960–2966.

[13]Delery, J. M., "Aspects of Vortex Breakdown," *Progress in Aerospace Sciences*, Vol. 30, No. 1, 1994, pp. 1–59.

[14]McCormick, B. W., *Aerodynamics, Aeronautics and Flight Mechanics,* 2nd ed., Wiley, New York, 1995, p. 138.

[15]Hoeijmakers, H. W. M., "Methods for Numerical Simulation of Leading-Edge Vortex Flow," *Studies of Vortex Dominated Flows,* edited by M. Y. Hussaini and M. D. Salas, Springer–Verlag, New York, 1985, pp. 223–269.

[16]Agrawal, S., Barnett, R. M., and Robinson, B. A., "Numerical Investigation of Vortex Breakdown on a Delta Wing, " *AIAA Journal*, Vol. 30, No. 3, 1992, pp. 584–591.

[17]Robinson, B. A., Barnett, R. M., and Agrawal, S., "Simple Numerical Criterion for Vortex Breakdown," *AIAA Journal*, Vol. 32, No. 1, 1994, pp. 116–122.

[18]Visbal, M. R., "Computed Unsteady Structure of Spiral Vortex Breakdown on Delta Wings," AIAA Paper 96-2074, 1996.

[19]Traub, L. W., "Simple Prediction Method for Location of Vortex Breakdown on Delta Wings," *Journal of Aircraft,* Vol. 33, No. 2, 1996, pp. 452–454.

[20]Traub, L. W., "Prediction of Vortex Breakdown and Longitudinal Characteristics of Swept Slender Planforms," *Journal of Aircraft,* Vol. 34, No. 3, 1997, pp. 353–359.

[21]Brandt, S. A., "Vortex Burst Model for the Vortex Lattice Method," *Journal of Aircraft,* Vol. 32, No. 6, 1995, pp. 1394–1396.

[22]Mahesh, K., "A Model for the Onset of Breakdown in an Axisymmetric Compressible Vortex," *Physics of Fluids*, Vol. 8, No. 12, 1996, pp. 3338–3345.

[23]Benjamin, B. T., "Theory of the Vortex Breakdown Phenomenon," *Journal of Fluid Mechanics,* Vol. 14, Pt. 4, 1962, pp. 495–515.

[24]Randall, J., and Leibovich, S., "The Critical State: A Trapped Wave Model of Vortex Breakdown," *Journal of Fluid Mechanics,* Vol. 58, Pt. 3, 1973, pp. 495–515.

[25]Leibovich, S., and Kribus, A., "Large Amplitude Wavetrains and Solitary Waves in Vortices," *Journal of Fluid Mechanics,* Vol. 216, July 1990, pp. 459–504.

[26]Keller, J. J., Egli, W., and Exley, W., "Force- and Loss-Free Transitions Between Flow States," *Journal of Applied Mathematics and Physics (ZAMP)*, Vol. 36, Oct. 1985, pp. 854–889.

[27]Hall, M. G., "Vortex Breakdown," *Annual Review of Fluid Mechanics,* Vol. 4, 1972, pp. 195–217.

[28]Buntine, J. D., and Saffman, P. G., "Inviscid Swirling Flows and Vortex Breakdown," *Proceedings of Royal Society of London*, Vol. 449, 1995, pp. 139–153.

[29]Lessen, H., Singh, P. J., and Paillet, P., "The Stability of a Trailing Line Vortex, Part 1: Inviscid Theory," *Journal of Fluid Mechanics,* Vol. 63, Pt. 4, 1974, pp. 753–763.

[30]Leibovich, S., and Stewartson, K., "A Sufficient Condition for the Instability of Columnar Vortices," *Journal of Fluid Mechanics,* Vol. 126, Jan. 1983, pp. 335–356.

[31]Brown, G. L., and Lopez, J. M., "Axisymmetric Vortex Breakdown, Part 2: Physical Mechanisms," *Journal of Fluid Mechanics,* Vol. 221, Dec. 1990, pp. 553–576.

[32]Wang, S., and Rusak, Z., "The Dynamics of a Swirling Flow in a Pipe and Transition to Axisymmetric Vortex Breakdown," *Journal of Fluid Mechanics,* Vol. 340, June 1997, pp. 177–223.

[33]Wang, S., and Rusak, Z., "On the Stability of an Axisymmetric Rotating Flow," *Physics of Fluids*, Vol. 8, No. 4, 1996, pp. 1007–1016.

[34]Rusak, Z., Wang, S., and Whiting, C., "The Evolution of a Perturbed Vortex in a Pipe to Axisymmetric Vortex Breakdown," *Journal of Fluid Mechanics,* Vol. 366, July 1998, pp. 211–237.

[35]Wang, S., and Rusak, Z., "The Effect of Slight Viscosity on Near Critical Swirling Flows," *Physics of Fluids,* Vol. 9, No. 7, 1997, pp. 1914–1927.

[36]Rusak, Z., Judd, K. P., and Wang, S., "The Effect of Small Pipe Divergence on Near Critical Swirling Flows," *Physics of Fluids,* Vol. 9, No. 8, 1997, pp. 2273–2285.

[37]Rusak, Z., "The Interaction of Near-Critical Swirling Flows in a Pipe with Inlet Vorticity Perturbations," *Physics of Fluids,* Vol. 10, No. 7, 1998, pp. 1672–1684.

[38]Rusak, Z., Whiting, C. H., and Wang, S., "Axisymmetric Breakdown of a Q-Vortex in a Pipe," *AIAA Journal*, Vol. 36, No. 10, 1998, pp. 1848–1953.

[39]Lamb, D., "Prediction of Vortex Breakdown in Leading-Edge Vortices Above Slender Delta Wings," M.Sc. Thesis, Dept. of Mechanical Engineering, Aeronautical Engineering and Mechanics, Rensselaer Polytechnic Inst., Troy, NY, 1998.